ACS APPLIED MATERIALS & INTERFACES

www.acsami.org

Research Article

Immobilization of Adenosine Derivatives onto Cellulose Nanocrystals via Click Chemistry for Biocatalysis Applications

Célestin Bourgery,[§] David Joram Mendoza,[§] Gil Garnier, Louis M. M. Mouterde,[*,§] and Florent Allais[*,§]

Cite This: *ACS Appl. Mater. Interfaces* 2024, 16, 11315−11323

Read Online

ACCESS | Metrics & More | Article Recommendations | Supporting Information

ABSTRACT: Adenosine triphosphate (ATP) is a central molecule of organisms and is involved in many biological processes. It is also widely used in biocatalytic processes, especially as a substrate and precursor of many cofactors—such as nicotinamide adenine dinucleotide phosphate (NADP(H)), coenzyme A (CoA), and *S*-adenosylmethionine (SAM). Despite its great scientific interest and pivotal role, its use in industrial processes is impeded by its prohibitory cost. To overcome this limitation, we developed a greener synthesis of adenosine derivatives and efficiently selectively grafted them onto organic nanoparticles. In this study, cellulose nanocrystals were used as a model combined with click chemistry via a copper-catalyzed azide/alkyne cycloaddition reaction (CuAAC). The grafted adenosine triphosphate derivative fully retains its biocatalytic capability, enabling heterobiocatalysis for modern biochemical processes.

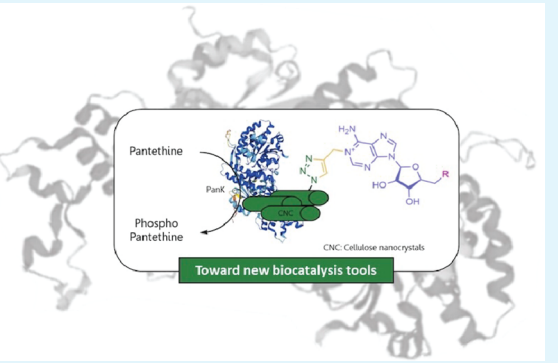

KEYWORDS: *ATP immobilization, biocatalysis, cofactor, nanocellulose, CNCs, click-chemistry*

INTRODUCTION

First isolated by Lohmann, Fiske, and SubbaRow in 1929,[1] adenosine triphosphate (ATP) is a coenzyme present in all living organisms that is central in the intra- or extracellular processes transferring energy to cells.[2] ATP derivatives have been widely studied as therapeutic strategy for COVID-19,[3] activated prodrug system for on-demand treatment of bacterial infections,[4] and for nucleotide metabolism.[5] ATP has been implemented in biocatalytic processes[6−8] such as kinase-cGAS cascade to synthesize a therapeutic STING activator,[9] amide synthesis,[10] or the novel STING antagonist MK-1454 synthesis.[11] To limit the stochiometric use of ATP in these reactions, more robust methods for its recycling are needed.[12] ATP also plays a major role as a precursor of many important cofactors, including coenzyme A (CoASH), *S*-adenosylmethionine (SAM), nicotinamide adenine dinucleotide NAD(H), and its phosphorylated form NADP(H).[13,14] Unfortunately, the high cost of these adenosine-based components has limited the development of cofactor-dependent enzymes industrially for biocatalytic processes. Considerable efforts have focused on optimizing their synthesis, regeneration and purification.[15−17] For instance, novel synthetic chemo-enzymatic route to coenzyme A (CoASH) and its disulfite derivate (CoAS),[2] as well as a membrane process for high-purity CoA and $NADP^+$ cofactors, have been reported.[18−20]

Immobilizing these cofactors would greatly facilitate their recovery and regeneration, increasing reaction speed, simplifying separation process, and reducing cost.[21,22] Moreover, this approach would enable continuous and heterogeneous industrial biocatalytic processes.[23,24] However, the immobilization of ATP-based cofactors remains challenging. Indeed, not only their numerous reactive groups are a serious obstacle to a selective grafting, but also structural modifications may alter their specific stereo positioning into the enzyme's binding site, thus potentially reducing or—even worse—inhibiting their activity.

Several research groups have proposed the use of these immobilized cofactors, particularly nicotinamide derivatives, for various applications. Lowe et al.[25] reported the purification of nicotinamide nucleotide-dependent dehydrogenases on immobilized cofactors, while Anithaa et al.[26] described the synthesis of gamma-irradiated EDTA-WO_3-modified GCE-immobilized NAD for electrode fabrication. However, very few studies have developed green syntheses, and mostly relied on synthetic approaches requiring multiple atom-consuming protections and substrate deprotection steps. To the best of our knowledge, no functional immobilized ATP or cofactors for applications in biocatalysis have been reported.[25]

Herein, we describe a greener, simple, and inexpensive synthetic route for immobilizing ATP onto cellulose nanocrystals (CNC). This robust proof-of-concept can be adapted

Received: December 22, 2023
Revised: January 31, 2024
Accepted: February 8, 2024
Published: February 23, 2024

for families of coenzymes sharing the same backbone such as CoASH or NADP(H). Two different routes are investigated to graft alkyne linkers of different sizes and structure. The immobilization of these adenosine derivatives by click chemistry on azide-functionalized CNCs was then achieved by a copper-catalyzed cycloaddition (CuAAC) reaction. The new materials were characterized by Fourier-transform infrared (FTIR) spectroscopy, elemental analysis, and X-ray photoelectron spectroscopy (XPS). The immobilized cofactor was finally tested in a biocatalytic process. This grafting strategy supports emerging applications in the medical field, including development of NLRP inflammasomes, progress in extracellular ATP in biological processes, and the engineering of new biocatalytic heterogeneous processes.[27−29]

RESULTS AND DISCUSSION

Click chemistry reactions are widely used in biochemistry (bioconjugation)[30,31] medicinal chemistry, and pharmaceuticals[32,33] due to the rapid generation of selective and stable bonds with no byproduct generation, therefore requiring no purification steps. Medical applications of click chemistry include the evaluation of anticancer, antiviral, and antimicrobial activity. Click chemistry reactions are also ideal for applications in materials science and the specific functionalization of surfaces.[34,35]

This is true with nanocellulose (CNC), a renewable, biodegradable, and the cheapest and most abundant type of organic nanoparticle that has excellent mechanical and chemical surface properties. The reactive hydroxyl groups on the cellulose surface can be easily modified with a wide range of functionalities. Click chemistry applications[36−38] have been reported, including a novel synthetic route for decorating cellulose nanocrystals with UV-absorbing phenolic esters,[39−41] and a thermoreversible nanofibrillar supramolecular hydrogel for the growth and release of cancer spheroids.[42] Here, the synthesis of grafted alkyne adenosine derivatives on CNC-N_3 nanocellulose using copper-catalyzed cycloaddition click chemistry is investigated.[43,44]

SYNTHESIS OF MODIFIED ALKYNE ADENOSINE, AMP, AND ATP

As CuAAC reaction requires azide and alkyne moieties to form a triazole ring, the synthesis of modified adenosine, AMP, and ATP containing an alkyne linker was first investigated (Figure 1). We applied the principles of green chemistry, without using or generating toxic products or solvents. Two different synthetic procedures were tested to obtain different types of alkyne linkers: (i) an aromatic electrophilic substitution using an excess of propargyl bromide in the cellulose-derived green solvent Cyrene (Figure 1, pathway 1), and (ii) through a ring-opening reaction between ATP and glycidyl propargyl ether (GPE) (Figure 1, pathway 2).

In the first route, the synthesis of unprotected substrate 1-*N*-propargylated adenosine described by Atdjian et al.[45] was performed as a model reaction to implement an aromatic electrophilic substitution using an excess of propargyl bromide in DMF at 50 °C for 24 h. DMF was then replaced by REACH-compliant Cyrene, a green nontoxic and aprotic polar solvent (Figure 1)[46] for a greener synthesis. The reaction provided the desired product, validating the proof of concept for the substitution of DMF with Cyrene in this reaction (Figures S1a and S5). Nevertheless, this methodology needs to

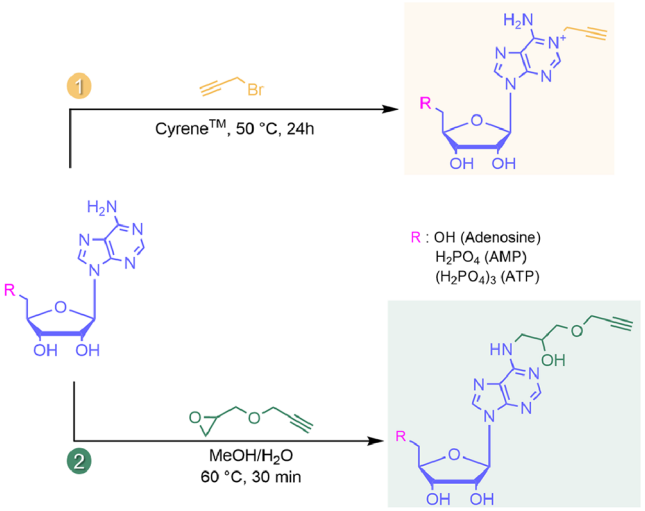

Figure 1. Synthesis of alkyne-modified adenosine derivatives: (1) aromatic electrophilic substitution using excess propargyl bromide in Cyrene, and (2) ring-opening reaction with glycidyl propargyl ether (GPE) in methanol/water.

be further optimized to reach yield similar or higher to the DMF-based one.[47−49] This synthetic strategy was then extended to AMP to confirm that phosphate groups do not hinder the condensation, before being applied to ATP. The successful grafting of the propargyl moiety for both AMP and ATP was confirmed by FTIR analysis, thus demonstrating that phosphate moieties were not deleterious for the reaction.

Inspired by the work of Shao et al., we developed a second route that allows a rapid and simple access to modified ATP with a variety of linkers[50] through a ring-opening reaction between ATP and GPE in a mixture of methanol and water (Figure 1, pathway 2). The reaction was confirmed by FTIR with the characteristic peak of the alkyne moiety at 2110 cm^{-1} (Figures S1c and S4).

GRAFTING ADENOSINE DERIVATIVES ONTO CNC BY CLICK CHEMISTRY

The synthesis and characterization of the grafted adenosine derivatives followed our previous study where we grafted phenolic compounds with an alkyne moiety onto CNC azide (CNC-N_3).[39] The synthesis was performed by activation of the primary hydroxy groups of CNCs by tosylation, followed by nucleophilic substitution of the resulting tosylates with azide groups (Figure 2a, pathway 1). Azidation was confirmed by FTIR with the appearance of a sharp stretching band at 2110 cm^{-1} (Figure 2b).

Although the synthetic pathway provided the targeted products in good yield, we aimed at developing a faster and pyridine-free alternative route under milder temperature conditions, while allowing the grafting of azide linkers of different natures and length. To do so, a two-step pathway consisting in the synthesis of 3-(azidopropyl)triethoxysilane from 3-(chloropropyl)triethoxysilane, followed by its functionalization on CNC under alkaline conditions was developed (Figure 2a, pathway 2).[51] FTIR analysis confirmed grafting of the N_3 linker with the presence of the characteristic azide peak at 2110 cm^{-1} (Figure 2b).

With the CNC-N_3 from route 1 in Figure 2, we then proceeded with the click chemistry reactions to graft the alkyne-modified compounds (i.e., adenosine, AMP, and ATP)

https://doi.org/10.1021/acsami.3c19025
ACS Appl. Mater. Interfaces 2024, 16, 11315−11323

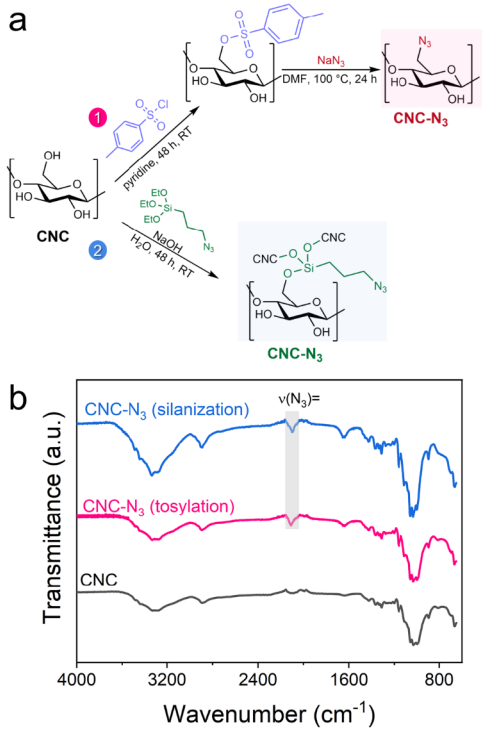

Figure 2. Azidation of CNCs. (a) Synthesis of CNC-N_3 was achieved via (1) tosylation, and (2) silanization. (b) FTIR spectra of CNC and CNC-N_3 synthesized via tosylation and silanization.

(Figure 3a). FTIR analysis of the resulting materials demonstrates the successful grafting shown by the ~70% decrease in the characteristic azide peak at 2110 cm^{-1} (Figure 3b). This is consistent with the literature and our previous studies of CuAAC reactions of nitrogen-containing CNCs, where a 50−70% reduction in the azide intensity was reported. The yield achieved is equivalent to the best conversion reported.[39,52−54]

The surface charge of the CNC-adenosine derivatives was quantified by the zeta potential in water (Figure S2). Adenosine-grafted CNCs exhibit zeta potentials of −20 to −30 mV, which confirm the stability of the materials in water and that the highly negative charge of CNCs was preserved after the click reaction. These grafted CNCs, however, are not as colloidally stable as the pristine CNCs (−50 mV) as a consequence of successful functionalization. DLS analysis also showed that the hydrodynamic diameters of pristine CNC and CNC-ATP in water are 103.3 ± 2.2 nm and 216.2 ± 19.2 nm, respectively. This indicates that CNC-ATP slightly aggregates in water and confirms the reduced dispersibility of CNC after ATP grafting.

XPS analysis further confirmed the grafting of the adenosine derivatives onto CNCs (Figure 4). Survey scans (Figure 4a) of pristine CNC and the grafted CNCs show carbon (287 eV) and oxygen (533 eV) as the major elements, as expected in cellulosic materials. Interestingly, the functionalization of azide and adenosine derivatives on CNCs introduced a nitrogen peak at 400−405 eV. Further, phosphorus peaks at 131−142 eV were observed from the survey scans of CNC-AMP and CNC-ATP, indicating that the phosphate groups were still intact. Figure 4b,c shows the high-resolution N 1s spectra of CNC-N_3 and CNC-Ade. The three peaks attributed to azide groups—N^+ azide, N azide, and N^- azide—at around 398.8, 400.5, and 404.5 eV, respectively, were observed in the N 1s spectrum of CNC-N_3 (Figure 4b). On the contrary, a broad peak at 398−406 eV was observed after the click reaction. This broad peak was deconvoluted into three major peaks: 401.5 eV attributed to the closely related N environments of 1,2,3-triazole ring and 399.2 and 403.8 eV, which likely correspond to the -NH_2 and N1/N2 of adenosine.[55] In addition, the P 2p spectrum (Figure 4d,e) showed two peaks at 134.5 and 137.9 eV, representing the P−O−C bond and the phosphate groups, respectively.[56−58] These data confirm the grafting of the compounds by click chemistry onto the CNCs.

Elemental analysis was used to determine the N/C ratio of the pristine CNC, CNC-N_3, and grafted CNCs (Figure 5 and Table S1). The N/C ratio of CNC after the click reaction increases as more nitrogenous compounds are functionalized. Similar to XPS analysis, phosphorus was significantly detected

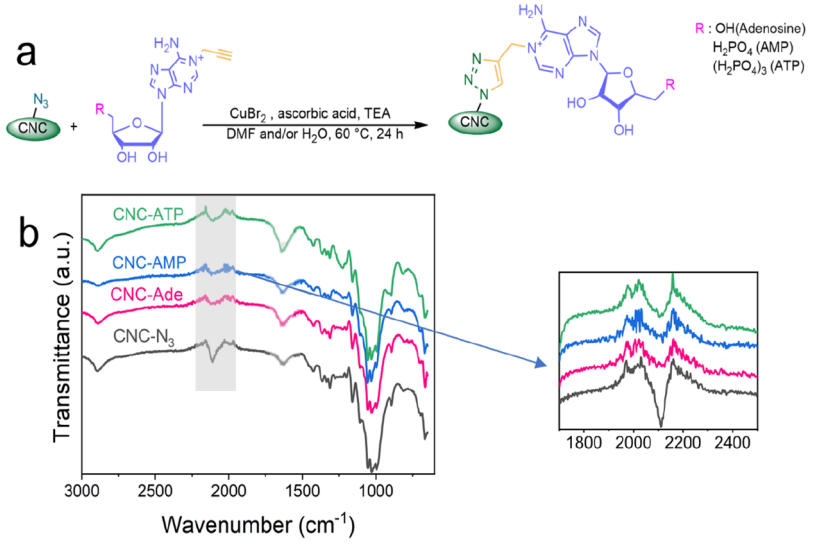

Figure 3. Synthesis of CNCs decorated with adenosine derivatives. (a) CuAAC reaction between CNC-N_3 and propargyl adenosine derivatives. (b) FTIR spectra of CNC-N_3 and click products (CNC-Ade, CNC-AMP, and CNC-ATP). Inset shows their transmittance bands at around 2100 cm^{-1}.

https://doi.org/10.1021/acsami.3c19025
ACS Appl. Mater. Interfaces 2024, 16, 11315−11323

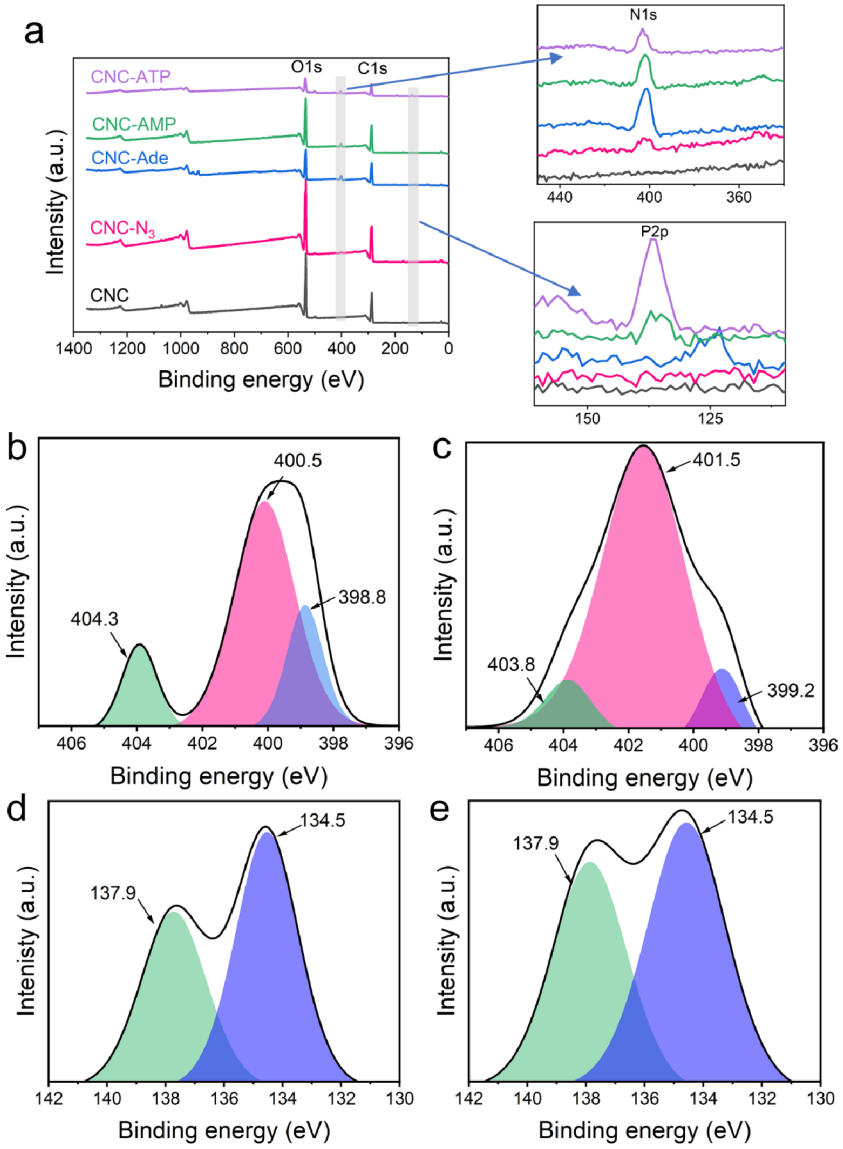

Figure 4. (a) Survey scans of CNC, CNC-N_3, and the click products. Insets show the binding energy peaks of N 1s and P 2p electrons. High resolution N 1s scans of (b) CNC-N_3 and (c) CNC-Ade. High-resolution P 2p scans of (d) CNC-AMP and (e) CNC-ATP.

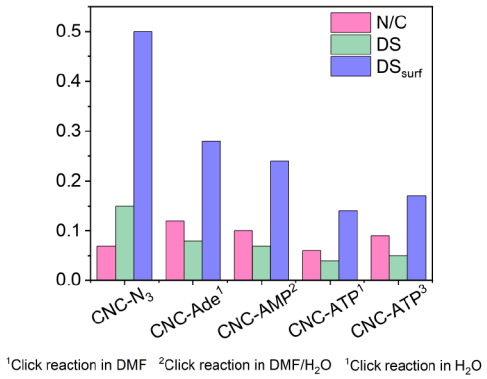

Figure 5. N/C ratio, DS, and DS_{surf} of CNC-N_3 and CNC-adenosine derivatives synthesized in different solvent systems.

from CNC-AMP and CNC-ATP, confirming that the phosphate groups are intact with the CNC. The degree of substitution (DS) and degree of surface substitution (DS_{surf}) were also quantified from elemental analysis. DS refers to the number of hydroxyl groups present per cellulosic glucosidic unit that were replaced by a substituent group, while DS_{surf} represents the number of hydroxyl groups per anhydroglucose unit (AGU) modified on the nanocrystal surface. DS was related to DS_{surf} using the chain ratio (Rc) or the ratio of the surface and total number of cellulose chains in CNC (eq 2). The number of surface (57) and total (201) chains were estimated using CNC rectangular rods with average dimensions of 8.6 × 7.7 nm^2 and lattice parameters of the cellulose Iβ unit cell, a = 0.61 nm and b = 0.54 nm. The azidation reaction is highly efficient, as the DS and DS_{surf} achieved are 0.15 and 0.5, respectively. These correspond to the maximum theoretical substitution of hydroxyl groups on CNCs.[52,53] The grafted CNCs achieved DS and DS_{surf} ranging from 0.09−0.12 and 0.14−0.28, respectively; these DS are similar to those reported for phenolic grafting.[39] These correspond to 28% to 56% conversion of the azide groups by their triazole derivatives and agree with FTIR analysis. However, a DS_{surf} > 1 is unlikely due to the limited reactivity of the C2 and C3 hydroxyl groups. The incomplete conversion

https://doi.org/10.1021/acsami.3c19025
ACS Appl. Mater. Interfaces 2024, 16, 11315−11323

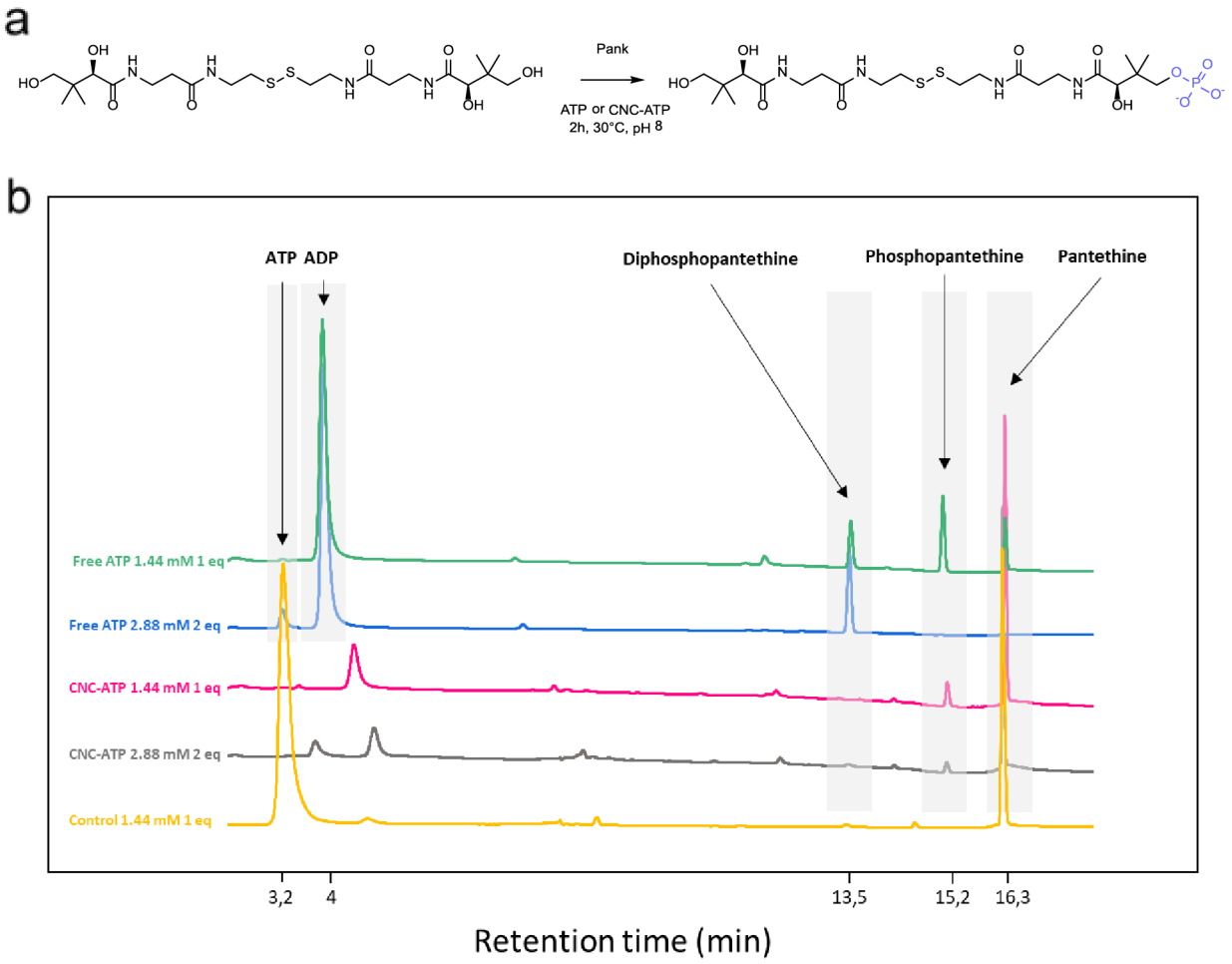

Figure 6. (a) PanK-mediated phosphopantethine synthesis with free ATP or ATP immobilized on CNC (CNC-ATP) as a phosphate donor. (b) HPLC analysis highlights the success of the reaction in the presence of phosphopantethine.

was expected as the steric congestion caused by the bulky adenosine molecules prevents direct access of the reactants to many of the functionalized CNC sites.

For a greener synthesis and higher solubility, DMF was replaced with water in the click reaction. We first demonstrated the feasibility of the concept using a 1:1 mixture of H_2O/DMF, before the reaction was completely carried out in water. The N/C ratios of the resulting materials from XPS surface analysis are reported in Supporting Information Table S2. For each compound, the N/C ratio measured is significantly higher for the reaction achieved using a mixture of H_2O/DMF or in water. The ratio was up to 3 times higher between a reaction in DMF or in a ratio (1:1) H_2O/DMF for CNC-Ade grafting. CNC-AMP has a N/C ratio 4 times greater in water and almost 60 times greater when the CNC-ATP reaction was carried out in a (1:1) H_2O/DMF mixture rather than pure DMF.

These higher grafting results are explained by improved solubilization of the compounds during the reaction and demonstrate an environmentally friendly route to graft CNCs. This synthesis in water and Cyrene can be further optimized and easily adapted to the immobilization of cofactors with the same purine core, opening new possibilities for SAM, NAD(H), NADP(H), or even FAD and CoA immobilization.

BIOCATALYSIS

The recombinant enzyme Pantothenate kinase (PanK) was expressed and implemented in the biocatalytic process to access phosphopantethine via phosphate transfer. This well-known reaction was carried out with D-pantethine and free ATP as reference, before being implemented with ATP immobilized on CNCs (CNC-ATP) as a phosphate group donor (Figure 6a).

The appearance of both phosphopantethine, the expected synthesis product, and diphosphopantethine in the HPLC analysis confirmed the success of the reaction with both free and immobilized substrates (Figure 6b). It is noteworthy to mention that, in the latter case, a second control experiment has been conducted to prove that there was no free ATP adsorbed on the CNC-ATP (Figure S6), demonstrating that the production of diphosphopantethine and phosphopantethine was exclusively due to the immobilized ATP. Although the reaction is less efficient with the immobilized ATP (39% vs 83% conversion pantethine with the free ATP), this first attempt demonstrates the proof of concept and highlights immobilized ATP nanomaterial as a phosphate-donating substrate. Immobilized ATP could enable easy regeneration and recycling of ATP in biocatalytic processes. The new immobilized nanomaterials investigated herein can be extended to many other biocatalytic reactions such as enzymatic preparation strategies for ATP-dependent synthetic

https://doi.org/10.1021/acsami.3c19025
ACS Appl. Mater. Interfaces 2024, 16, 11315−11323

processes (e.g., production of SAM, CoASH),[18,59] *in vitro* ATP regeneration systems,[60] or for the synthesis of dihydroxyacetone phosphate (DHAP),[61] glucose-6-phosphate (G6P),[62] and fructose-6-phosphate (F6P).[63] It opens new prospects for the immobilization of adenosine derivative cofactors by green synthesis on CNCs for biocatalytic processes. Our previous study on the grafting of UV filters on CNC showed that the residual amounts of copper in phenolic-ester-grafted CNCs caused a cytotoxic effect on murine fibroblast cells after 24 h. We expect that the presence of copper ions could detrimentally affect the ATP-mediated reaction, as well. Thus, the removal of residual copper from CNCs after the click reaction is important for this application. In this aim, copper ions were substantially removed by dialyzing the grafted CNCs against water for 5 days.

CONCLUSION

We have demonstrated a new route for the immobilization of adenosine derivatives on cellulose nanocrystals (CNC) using the classical copper-catalyzed azide−alkyne cycloaddition (CuAAC) reaction. We also showed the biocatalysis ability of the ATP-functionalized CNC. Adenosine derivatives, including ATP, carrying alkyne linkers of varying nature and length, were efficiently prepared by green chemistry. Azide-bearing CNCs were efficiently prepared by using a well-established procedure involving the selective tosylation of the primary alcohols followed by the subsequent substitution of the resulting tosylates with azides. Aiming at greener methodologies, a much faster and pyridine-free approach was also demonstrated for surface modifications of CNCs via silanization ($(EtO)_3Si\text{-}(CH_2)_3\text{-}N_3$, NaOH) in water. These functionalized adenosine derivatives were then efficiently grafted on azide-bearing CNC using a classical procedure in DMF. The combination of FTIR spectroscopy, XPS and elemental analysis confirmed the successful cycloaddition of azides-grafted cellulose nanocrystals (CNC-N_3) modified with azides and alkyne analogues of adenosine derivatives. Immobilized ATP was then implemented in a biocatalytic reaction in the presence of recombinant PanK and D-pantethine to successfully access phosphopantethine. Such cellulose nanocrystals are thus promising sustainable nanomaterials that can be used as new biocatalytic tools to facilitate cofactor recycling and regeneration, or as biocatalyst for heterogeneous or flow-through reactor.

METHODS

Chemicals. Freeze-dried cellulose nanocrystals (sulfuric acid-hydrolyzed, 0.9% S) were purchased from the University of Maine, USA. Copper(II) bromide ($CuBr_2$), potassium carbonate (K_2CO_3), 3-(chloropropyl)triethoxysilane, and *p*-toluenesulfonyl chloride were purchased from Sigma-Aldrich. Absolute ethanol and *N*,*N*-dimethylformamide (DMF) were acquired from Ajax FineChem. Propargyl bromide (80 wt % in toluene) and sodium azide (NaN_3) were purchased from Acros Organics, and ascorbic acid and triethylamine were purchased from Alfa Aesar. AMP (TCI, > 98%), ATP (Acros Organics, 98%), adenine (TCI > 99%), and D-pantethine (abcr, 95%, syrup) were also obtained. Cyrene (dihydrolevoglucosenone)—which could be obtained from lignocellulosic biomass such as sawdust—was received from Circa Group.

Synthesis of Modified Adenosine, AMP, and ATP Containing an Alkyne Moiety. Modified adenosine and AMP were synthesized according the method of Atdjian et al.[45] with some modifications. Propargyl bromide (80%w in toluene) (143 μL, 1.8 mmol) was added to a solution of adenosine (100 mg, 0.37 mmol) in DMF or Cyrene (1 mL), and water was added until homogenization was reached. The reaction mixture was stirred at 50 °C for 24 h. The crude product was then evaporated under vacuum. A pastelike mixture was then obtained and analyzed by FTIR spectroscopy.

A second method was used based on the work of Shao et al.[50] for the synthesis of modified ATP. ATP (20 mg) and glycidyl propargyl ether (GPE) (10 μL) were added to a solution composed of 2 mL of H_2O and 2 mL of MeOH. The solution was then sonicated for 10 min and placed at 60 °C for 30 min, allowing the amino groups of ATPs to react with the epoxy moiety of GPE. The final product was then analyzed by FTIR.

Surface Tosylation and Azidation of Cellulose Nanocrystals. Surface tosylation and azidation reactions of CNCs were performed following the same procedure as presented in a previous study.[39] CNCs (5.0 g, 30.85 mmol anhydroglucose unit (AGU)) were suspended in 100 mL of pyridine and cooled to 10 °C. *p*-Toluenesulfonyl chloride (9 g, 50 mmol) was slowly added, and the reaction mixture was stirred at room temperature for 48 h. CNCs were precipitated by the addition of 200 mL of ethanol followed by centrifugation at 11 000 rpm for 20 min. The particles were subsequently washed five times each with ethanol and water and freeze-dried for 2 days to provide surface-tosylated CNCs (CNC-Tos) in 94% yield.

Approximately 0.9 g of CNC-Tos (1 equiv) suspended in 50 mL of DMF was reacted with 0.9 g (1 equiv) of sodium azide. The reaction was stirred at 100 °C for 24h. Similarly, CNCs were isolated by the addition of 200 mL of ethanol followed by repeated centrifugation (11 000 rpm, 20 min) and washing with ethanol and water. The particles resuspended in water were dialyzed against Milli-Q water for 5 days and freeze-dried for 2 days. Surface-azidized CNCs (CNC-N_3) were obtained in 96% yield (0.86 g).

A second protocol was also performed for the synthesis of CNC-N_3 using 3-(chloropropyl)triethoxysilane. For this, 3-(chloropropyl)triethoxysilane (5 g, 0.02 mol) and sodium azide (2 g, 0.031 mol) were added in a 50 mL flask, before adding 21 mL of DMF. The reaction was stirred for 4 h at 60 °C. After extraction with ethyl acetate, the organic layer was washed 3 to 4 times with a saturated ammonium chloride solution and dried *in vacuo*. 200 μL (809 μmol) of 3-(azidopropyl)triethoxysilane was then added to CNC and the reaction was stirred at RT under stirring for 4 h. The reaction medium was diluted in distilled water to a final volume of 45 mL, before being successively washed with H_2O, EtOH, acetone, and H_2O at RT.[51]

NMR. ^1H NMR spectra were recorded on a Bruker Fourier 300 MHz (D_2O residual signal at 4.79 ppm).

Click Reaction of CNC-N_3 with Alkyne-Modified Adenosine, AMP, and ATP. The copper(I)-catalyzed cycloaddition reaction of alkyne derivatives of ATP with CNC-N_3 was adapted from a previous report,[40] with some modifications. Alkyne derivatives (1.7 g of the crude mixture obtained previously) and CNC-N_3 (0.4 g) were mixed in 40 mL DMF, in a H_2O/DMF mixture (1:1; 40 mL) or entirely in water (40 mL). A solution containing $CuBr_2$ (56 mg, 0.006 mol)), ascorbic acid (160 mg, 0.02 mol), and triethylamine (400 μL, 100 μmol) in DMF was then slowly added, and the

https://doi.org/10.1021/acsami.3c19025
ACS Appl. Mater. Interfaces 2024, 16, 11315−11323

reaction was allowed to proceed at 60 °C for 24 h. The crude product was isolated by ethanol precipitation (200 mL) followed by repeated centrifugation (11 000 rpm, 20 min) and washing with ethanol and water. The particles were dialyzed against Milli-Q water for 5 days and freeze-dried for 2 days.

CHARACTERIZATION OF THE CLICK PRODUCTS

FTIR Spectroscopy. Analysis and instruments (Fourier Transform Infrared (FTIR) spectrometer—Agilent Technologies Cary 630 FTIR—equipped with a diamond ATR accessory) were the same as those used in a previous study.[39] Freeze-dried samples were analyzed with 32 scans at 4 cm^{-1} resolution and were recorded in the range of 4000−500 cm^{-1}.

Elemental Analysis and DS. A Thermo Scientific FlashSmart CHNS analyzer was used to perform elemental analysis of pristine and functionalized CNCs. The DS of modified CNCs were quantified based on %*N* and calculated using eq 1 as previously reported:

$$DS = \frac{-\%N \times M_{AGU}}{\%N \times M_{graft} - Mn} \quad (1)$$

where %*N* is the weight percentage of nitrogen, M_{AGU} is the mass of anhydroglucose unit (162.14), *n* is the number of nitrogen atoms in the substituent group, and *M* is the molecular weight of the substituent group.

The DS_{surf} is based on the equation:

$$DS_{surf} = \frac{DS}{RC} \quad (2)$$

where RC is the assuming CNC chain ratio (Rc): 0.29.[39,54]

XPS. The Thermo Scientific Nexsa XPS spectrometer equipped with an Al−Kα irradiation source was used for chemical analysis of freeze-dried, pure, or modified CNCs surfaces. Survey scans were performed from 10 to 1350 eV with a scan step of 1 eV. High-resolution N 1s and P 2p spectra of 392−410 and 126−144 eV, respectively, were also recorded. All data processing and analyses were performed using the Thermo Avantage software, in the same way as in a previous study.[39]

Dynamic Light Scattering and Zeta Potential. The hydrodynamic diameter (D_h) and zeta potential of sonicated CNC and grafted-CNC aqueous dispersions were measured using a Brookhaven Nanobrook Omni particle analyzer. Measurements were performed five times for each sample, and the average is reported. All samples were diluted by 13.5× before measurement.

DEMONSTRATION OF THE ENZYMATIC ACTIVITY OF A KINASE ON THESE IMMOBILIZED COFACTORS

- ***Production of recombinant pantethine kinase (Pank).*** The method is the same as that used in a previous study.[18]
- ***Implementation of the enzyme and immobilized ATP in the biocatalytic reaction.*** The enzymatic reaction was carried out with D-pantethine (1.44 mM) and ATP (1 equiv) or CNC-ATP (1 equiv), in 2 mL of a buffer composed of 20 mM of KCl, 10 mM of $MgCl_2$, 50 mM of Tris, pH 8, PanK (15 μg). The reaction was carried out at 30 °C for 2 h. A reaction in the absence of the enzyme was performed as a first negative control.

A second negative control was also performed as follows: D-pantethine (1.44 mM) and CNC-ATP (1 equiv) were incubated, for 2 h at 30 °C, in 2 mL of a buffer composed of 20 mM of KCl, 10 mM of $MgCl_2$, 50 mM of Tris, pH 8. The solution was then filtered at 0.2 μm. Pank (15 μg) was added to the resulting filtrate and the mixture was incubated for an additional 2 h. The reactions were conducted in duplicate and analyzed by HPLC (Figure S6).

- ***HPLC methods.*** Chromatograms were recorded using a Thermo Scientific reversed-phase HPLC equipped with an Acclaim Polar Advantage II C18 column (150 × 4.6 mm, 3 μm particle size). The separation was performed at a flow rate of 1 $mL.min^{-1}$ over 25 min. The mobile phase was water [solvent A] and acetonitrile [solvent B] both supplemented with 50 mM NaH_2PO_4 [D]. The following elution gradient program was used: gradient: 1.2% [B] held 2.5 min, 1.2% to 7.2% [B] in 5 min, 7.2% to 11.2% [B] in 2.5 min, 11.2% to 20% [B] in 3 min, 20% to 30% [B] in 2 min, 30% [B] held 3 min, 30% back to 1.2% [B] in 2 min, 1.2% [B] held 5 min. Samples were analyzed at the following wavelengths: 220 and 260 nm.

Commercial standards ATP and D-panthethine were used to determine the retention times of these products.

ASSOCIATED CONTENT

Data Availability Statement

The data sets used and/or analyzed during the current study available from the corresponding author on reasonable request.

Supporting Information

The Supporting Information is available free of charge at https://pubs.acs.org/doi/10.1021/acsami.3c19025

FTIR spectra of adenosine derivatives; zeta potential of pristine and adenosine-, AMP- and ATP-grafted CNCs; NMR spectra of synthesized compounds and materials; second negative control for the biocatalytic assay (PDF)

AUTHOR INFORMATION

Corresponding Authors

Louis M. M. Mouterde − *URD Agro-Biotechnologies Industrielles (ABI), CEBB, AgroParisTech, Pomacle 51110, France;* orcid.org/0000-0002-4096-1629; Email: louis.mouterde@agroparistech.fr

Florent Allais − *URD Agro-Biotechnologies Industrielles (ABI), CEBB, AgroParisTech, Pomacle 51110, France; Bioresource Processing Research Institute of Australia (BioPRIA), Department of Chemical and Biological Engineering, Monash University, Clayton, VIC 3800, Australia;* orcid.org/0000-0003-4132-6210; Email: florent.allais@agroparistech.fr

Authors

Célestin Bourgery − *URD Agro-Biotechnologies Industrielles (ABI), CEBB, AgroParisTech, Pomacle 51110, France*

David Joram Mendoza − *Bioresource Processing Research Institute of Australia (BioPRIA), Department of Chemical and Biological Engineering, Monash University, Clayton, VIC 3800, Australia*

Gil Garnier − *Bioresource Processing Research Institute of Australia (BioPRIA), Department of Chemical and Biological Engineering, Monash University, Clayton, VIC*

https://doi.org/10.1021/acsami.3c19025
ACS Appl. Mater. Interfaces 2024, 16, 11315−11323

3800, Australia; URD Agro-Biotechnologies Industrielles (ABI), CEBB, AgroParisTech, Pomacle 51110, France; orcid.org/0000-0003-3512-0056

Complete contact information is available at: https://pubs.acs.org/10.1021/acsami.3c19025

Author Contributions

§C.B. and D.J.M. contributed equally. L.M.M.M. and F.A. contributed equally. C.B., L.M.M.M., and F.A. conceived the research. L.M.M.M., F.A., D.J.M., and G.G. supervised the research. C.B. performed all the experiments and analyses. L.M.M.M. and D.J.M. provided the technical guidelines. L.M.M.M., F.A., D.J.M., and G.G. reviewed the results. C.B. drafted the article. L.M.M.M., F.A., D.J.M., and G.G. reviewed, improved and approved the article. F.A. and G.G. acquired funding.

Notes

The authors declare no competing financial interest.

■ ACKNOWLEDGMENTS

This work was supported by the Région Grand Est, Conseil Départemental de la Marne and Grand Reims. C. Bourgery would like to thank BioPRIA of the Department of Chemical and Biological Engineering, Monash University for hosting him for 2 months. Many thanks to Y. Hora of Monash X-ray Platform (MXP) for the XPS analysis.

■ REFERENCES

(1) Maruyama, K. The Discovery of Adenosine Triphosphate and the Establishment of Its Structure. *J. Hist. Biol* **1991**, *24* (1), 145−154.
(2) Burton, K. Energy of Adenosine Triphosphate. *Nature* **1958**, *181* (4623), 1594−1595.
(3) Li, G.; Hilgenfeld, R.; Whitley, R.; De Clercq, E. Therapeutic Strategies for COVID-19: Progress and Lessons Learned. *Nat. Rev. Drug Discovery* **2023**, *22* (6), 449−475.
(4) Weng, Y.; Chen, H.; Chen, X.; Yang, H.; Chen, C.-H.; Tan, H. Adenosine Triphosphate-Activated Prodrug System for on-Demand Bacterial Inactivation and Wound Disinfection. *Nat. Commun.* **2022**, *13* (1), 4712.
(5) Mullen, N. J.; Singh, P. K. Nucleotide Metabolism: A Pan-Cancer Metabolic Dependency. *Nat. Rev. Cancer* **2023**, *23* (5), 275−294.
(6) Pfeiffer, M.; Ribar, A.; Nidetzky, B. A Selective and Atom-Economic Rearrangement of Uridine by Cascade Biocatalysis for Production of Pseudouridine. *Nat. Commun.* **2023**, *14* (1), 2261.
(7) Hartley, C. J.; Williams, C. C.; Scoble, J. A.; Churches, Q. I.; North, A.; French, N. G.; Nebl, T.; Coia, G.; Warden, A. C.; Simpson, G.; Frazer, A. R.; Jensen, C. N.; Turner, N. J.; Scott, C. Engineered Enzymes That Retain and Regenerate Their Cofactors Enable Continuous-Flow Biocatalysis. *Nat. Catal.* **2019**, *2* (11), 1006−1015.
(8) Bering, L.; Craven, E. J.; Sowerby Thomas, S. A.; Shepherd, S. A.; Micklefield, J. Merging Enzymes with Chemocatalysis for Amide Bond Synthesis. *Nat. Commun.* **2022**, *13* (1), 380.
(9) McIntosh, J. A.; Liu, Z.; Andresen, B. M.; Marzijarani, N. S.; Moore, J. C.; Marshall, N. M.; Borra-Garske, M.; Obligacion, J. V.; Fier, P. S.; Peng, F.; Forstater, J. H.; Winston, M. S.; An, C.; Chang, W.; Lim, J.; Huffman, M. A.; Miller, S. P.; Tsay, F.-R.; Altman, M. D.; Lesburg, C. A.; Steinhuebel, D.; Trotter, B. W.; Cumming, J. N.; Northrup, A.; Bu, X.; Mann, B. F.; Biba, M.; Hiraga, K.; Murphy, G. S.; Kolev, J. N.; Makarewicz, A.; Pan, W.; Farasat, I.; Bade, R. S.; Stone, K.; Duan, D.; Alvizo, O.; Adpressa, D.; Guetschow, E.; Hoyt, E.; Regalado, E. L.; Castro, S.; Rivera, N.; Smith, J. P.; Wang, F.; Crespo, A.; Verma, D.; Axnanda, S.; Dance, Z. E. X.; Devine, P. N.; Tschaen, D.; Canada, K. A.; Bulger, P. G.; Sherry, B. D.; Truppo, M. D.; Ruck, R. T.; Campeau, L.-C.; Bennett, D. J.; Humphrey, G. R.; Campos, K. R.; Maddess, M. L. A Kinase-CGAS Cascade to Synthesize a Therapeutic STING Activator. *Nature* **2022**, *603* (7901), 439−444.
(10) Wu, S.; Snajdrova, R.; Moore, J. C.; Baldenius, K.; Bornscheuer, U. T. Biocatalysis: Enzymatic Synthesis for Industrial Applications. *Angew. Chem. Int. Ed.* **2021**, *60* (1), 88−119.
(11) Benkovics, T.; Peng, F.; Phillips, E. M.; An, C.; Bade, R. S.; Chung, C. K.; Dance, Z. E. X.; Fier, P. S.; Forstater, J. H.; Liu, Z.; Liu, Z.; Maligres, P. E.; Marshall, N. M.; Salehi Marzijarani, N.; McIntosh, J. A.; Miller, S. P.; Moore, J. C.; Neel, A. J.; Obligacion, J. V.; Pan, W.; Pirnot, M. T.; Poirier, M.; Reibarkh, M.; Sherry, B. D.; Song, Z. J.; Tan, L.; Turnbull, B. W. H.; Verma, D.; Waldman, J. H.; Wang, L.; Wang, T.; Winston, M. S.; Xu, F. Diverse Catalytic Reactions for the Stereoselective Synthesis of Cyclic Dinucleotide MK-1454. *J. Am. Chem. Soc.* **2022**, *144* (13), 5855−5863.
(12) France, S. P.; Lewis, R. D.; Martinez, C. A. The Evolving Nature of Biocatalysis in Pharmaceutical Research and Development. *JACS. Au* **2023**, *3* (3), 715−735.
(13) Black, W. B.; Zhang, L.; Mak, W. S.; Maxel, S.; Cui, Y.; King, E.; Fong, B.; Sanchez Martinez, A.; Siegel, J. B.; Li, H. Engineering a Nicotinamide Mononucleotide Redox Cofactor System for Biocatalysis. *Nat. Chem. Biol.* **2020**, *16* (1), 87−94.
(14) Wang, X.; Feng, Y.; Guo, X.; Wang, Q.; Ning, S.; Li, Q.; Wang, J.; Wang, L.; Zhao, Z. K. Creating Enzymes and Self-Sufficient Cells for Biosynthesis of the Non-Natural Cofactor Nicotinamide Cytosine Dinucleotide. *Nat. Commun.* **2021**, *12* (1), 2116.
(15) Mordhorst, S.; Andexer, J. N. Round, round we go − strategies for enzymatic cofactor regeneration. *Nat. Prod. Rep.* **2020**, *37* (10), 1316−1333.
(16) Liu, W.; Wang, P. Cofactor Regeneration for Sustainable Enzymatic Biosynthesis. *Biotechnol. Adv.* **2007**, *25* (4), 369−384.
(17) Jaroensuk, J.; Chuaboon, L.; Chaiyen, P. Biochemical Reactions for in Vitro ATP Production and Their Applications. *Mol. Catal.* **2023**, *537*, 112937.
(18) Mouterde, L. M. M.; Stewart, J. D. An Efficient Chemoenzymatic Synthesis of Coenzyme A and Its Disulfide. *Org. Process Res. Dev.* **2016**, *20* (5), 954−959.
(19) Mouterde, L. M. M.; Willig, G.; Langlait, M. M. J.; Brunois, F.; Chadni, M.; Allais, F. Unlocking the Access to Oxidized Coenzyme A via a Single-Step Green Membrane-Based Purification. *Sci. Rep.* **2022**, *12* (1), 12991.
(20) Bourgery, C.; Willig, G.; Allais, F.; Mouterde, L. M. M. Combining the Power of Biocatalysis and Membrane-Based Purification To Access NADP+. *ACS Sustainable Chem. Eng.* **2023**, *11* (12), 4662−4669.
(21) Wang, Z.; Etienne, M.; Quilès, F.; Kohring, G.-W.; Walcarius, A. Durable cofactor immobilization in sol−gel bio-composite thin films for reagentless biosensors and bioreactors using dehydrogenases. *Biosens. Bioelectron.* **2012**, *32* (1), 111−117.
(22) Velasco-Lozano, S.; Benítez-Mateos, A. I.; López-Gallego, F. Co-Immobilized Phosphorylated Cofactors and Enzymes as Self-Sufficient Heterogeneous Biocatalysts for Chemical Processes. *Angew. Chem. Int. Ed.* **2017**, *56* (3), 771−775.
(23) Santis, P. D.; Meyer, L.-E.; Kara, S. The rise of continuous flow biocatalysis − fundamentals, very recent developments and future perspectives. *Reaction Chem. Eng.* **2020**, *5* (12), 2155−2184.
(24) Bolivar, J. M.; Eisl, I.; Nidetzky, B. Advanced Characterization of Immobilized Enzymes as Heterogeneous Biocatalysts. *Catal. Today* **2016**, *259*, 66−80.
(25) Lowe, C. R.; Harvey, M. J.; Craven, D. B.; Kerfoot, M. A.; Hollows, M. E.; Dean, P. D. G. The Purification of Nicotinamide Nucleotide-Dependent Dehydrogenases on Immobilized Cofactors. *Biochem. J.* **1973**, *133* (3), 507−513.
(26) Anithaa, A. C.; Asokan, K.; Lavanya, N.; Sekar, C. Nicotinamide Adenine Dinucleotide Immobilized Tungsten Trioxide Nanoparticles for Simultaneous Sensing of Norepinephrine, Melatonin and Nicotine. *Biosens. Bioelectron.* **2019**, *143*, 111598.
(27) Liao, K.-C.; Sandall, C. F.; Carlson, D. A.; Ulke-Lemée, A.; Platnich, J. M.; Hughes, P. F.; Muruve, D. A.; Haystead, T. A. J.;

MacDonald, J. A. Application of Immobilized ATP to the Study of NLRP Inflammasomes. *Archiv. Biochem. Biophys.* **2019**, *670*, 104−115.
(28) Agteresch, H. J.; Dagnelie, P. C.; van den Berg, J. W.; Wilson, J. H. Adenosine Triphosphate: Established and Potential Clinical Applications. *Drugs* **1999**, *58* (2), 211−232.
(29) Zhang, Q.; Song, B.; Xu, Y.; Yang, Y.; Ji, J.; Cao, W.; Lu, J.; Ding, J.; Cao, H.; Chu, B.; Hong, J.; Wang, H.; He, Y. In Vivo Bioluminescence Imaging of Natural Bacteria within Deep Tissues via ATP-Binding Cassette Sugar Transporter. *Nat. Commun.* **2023**, *14* (1), 2331.
(30) Presolski, S. I.; Hong, V. P.; Finn, M. G. Copper-Catalyzed Azide−Alkyne Click Chemistry for Bioconjugation. *Curr. Protoc. Chem. Biol.* **2011**, *3* (4), 153−162.
(31) Zheng, T.; Rouhanifard, S. H.; Jalloh, A. S.; Wu, P. Click Triazoles for Bioconjugation. *Top. Heterocycl. Chem.* **2012**, *28*, 163−183.
(32) Ernst, B.; Magnani, J. L. From Carbohydrate Leads to Glycomimetic Drugs. *Nat. Rev. Drug Discovery* **2009**, *8* (8), 661−677.
(33) He, X.-P.; Zeng, Y.-L.; Zang, Y.; Li, J.; Field, R. A.; Chen, G.-R. Carbohydrate CuAAC Click Chemistry for Therapy and Diagnosis. *Carbohydr. Res.* **2016**, *429*, 1−22.
(34) Decan, M. R.; Impellizzeri, S.; Marin, M. L.; Scaiano, J. C. Copper Nanoparticle Heterogeneous Catalytic 'Click' Cycloaddition Confirmed by Single-Molecule Spectroscopy. *Nat. Commun.* **2014**, *5* (1), 4612.
(35) Tian, R.; Xu, S.-M.; Xu, Q.; Lu, C. Large-Scale Preparation for Efficient Polymer-Based Room-Temperature Phosphorescence via Click Chemistry. *Sci. Adv.* **2020**, *6* (21), No. eaaz6107.
(36) Babi, M.; Fatona, A.; Li, X.; Cerson, C.; Jarvis, V. M.; Abitbol, T.; Moran-Mirabal, J. M. Efficient Labeling of Nanocellulose for High-Resolution Fluorescence Microscopy Applications. *Biomacromolecules* **2022**, *23* (5), 1981−1994.
(37) Zhou, L.; He, H.; Li, M.-C.; Huang, S.; Mei, C.; Wu, Q. Grafting Polycaprolactone Diol onto Cellulose Nanocrystals via Click Chemistry: Enhancing Thermal Stability and Hydrophobic Property. *Carbohydr. Polym.* **2018**, *189*, 331−341.
(38) Mujtaba, M.; Negi, A.; King, A. W. T.; Zare, M.; Kuncova-Kallio, J. Surface Modifications of Nanocellulose for Drug Delivery Applications; a Critical Review. *Curr. Opin. Biomed. Eng.* **2023**, *28*, 100475.
(39) Mendoza, D. J.; Mouterde, L. M. M.; Browne, C.; Singh Raghuwanshi, V.; Simon, G. P.; Garnier, G.; Allais, F. Grafting Nature-Inspired and Bio-Based Phenolic Esters onto Cellulose Nanocrystals Gives Biomaterials with Photostable Anti-UV Properties. *ChemSuschem* **2020**, *13* (24), 6460−6460.
(40) Mendoza, D. J.; Browne, C.; Raghuwanshi, V. S.; Mouterde, L. M. M.; Simon, G. P.; Allais, F.; Garnier, G. Phenolic Ester-Decorated Cellulose Nanocrystals as UV-Absorbing Nanoreinforcements in Polyvinyl Alcohol Films. *ACS Sustainable Chem. Eng.* **2021**, *9* (18), 6427−6437.
(41) Mendoza, D. J.; Maliha, M.; Raghuwanshi, V. S.; Browne, C.; Mouterde, L. M. M.; Simon, G. P.; Allais, F.; Garnier, G. Diethyl Sinapate-Grafted Cellulose Nanocrystals as Nature-Inspired UV Filters in Cosmetic Formulations. *Mater. Today Bio* **2021**, *12*, 100126.
(42) Li, Y.; Khuu, N.; Gevorkian, A.; Sarjinsky, S.; Therien-Aubin, H.; Wang, Y.; Cho, S.; Kumacheva, E. Supramolecular Nanofibrillar Thermoreversible Hydrogel for Growth and Release of Cancer Spheroids. *Angew. Chem. Int. Ed.* **2017**, *56* (22), 6083−6087.
(43) Creech, C.; Kanaujia, M.; Causey, C. P. Synthesis and Evaluation of 2-Ethynyl-Adenosine-5′-Triphosphate as a Chemical Reporter for Protein AMPylation. *Org. Biomol. Chem.* **2015**, *13* (31), 8550−8555.
(44) Castro, V.; Rodríguez, H.; Albericio, F. CuAAC: An Efficient Click Chemistry Reaction on Solid Phase. *ACS Comb. Sci.* **2016**, *18* (1), 1−14.
(45) Atdjian, C.; Coelho, D.; Iannazzo, L.; Ethève-Quelquejeu, M.; Braud, E. Synthesis of Triazole-Linked SAM-Adenosine Conjugates: Functionalization of Adenosine at N-1 or N-6 Position without Protecting Groups. *Molecules* **2020**, *25* (14), 3241.
(46) *Cyrene - Circa Group AS. Circa Group AS - Changing chemistry for good*^{TM}. https://circa-group.com/products/cyrene/ (accessed 2023−06−14).
(47) Camp, J. E. Bio-Available Solvent Cyrene: Synthesis, Derivatization, and Applications. *ChemSuschem* **2018**, *11* (18), 3048−3055.
(48) Sherwood, J.; Bruyn, M. D.; Constantinou, A.; Moity, L.; McElroy, C. R.; Farmer, T. J.; Duncan, T.; Raverty, W.; Hunt, A. J.; Clark, J. H. Dihydrolevoglucosenone (Cyrene) as a Bio-Based Alternative for Dipolar Aprotic Solvents. *Chem. Commun.* **2014**, *50* (68), 9650−9652.
(49) Stini, N. A.; Gkizis, P. L.; Kokotos, C. G. Cyrene: A Bio-Based Novel and Sustainable Solvent for Organic Synthesis. *Green Chem.* **2022**, *24* (17), 6435−6449.
(50) Shao, H.; Lai, L.; Xu, D.; Crommen, J.; Wang, Q.; Jiang, Z. Development of Zirconium Modified Adenosine Triphosphate Functionalized Monolith for Specific Enrichment of N-Glycans. *J. Chromatogr. A* **2021**, *1644*, 462090.
(51) Hettegger, H.; Beaumont, M.; Potthast, A.; Rosenau, T. Aqueous Modification of Nano- and Microfibrillar Cellulose with a Click Synthon. *ChemSuschem* **2016**, *9* (1), 75−79.
(52) Eyley, S.; Shariki, S.; Dale, S. E. C.; Bending, S.; Marken, F.; Thielemans, W. Ferrocene-Decorated Nanocrystalline Cellulose with Charge Carrier Mobility. *Langmuir* **2012**, *28* (16), 6514−6519.
(53) Feese, E.; Sadeghifar, H.; Gracz, H. S.; Argyropoulos, D. S.; Ghiladi, R. A. Photobactericidal Porphyrin-Cellulose Nanocrystals: Synthesis, Characterization, and Antimicrobial Properties. *Biomacromolecules* **2011**, *12* (10), 3528−3539.
(54) Eyley, S.; Thielemans, W. Surface Modification of Cellulose Nanocrystals. *Nanoscale* **2014**, *6* (14), 7764−7779.
(55) Peeling, J.; Hruska, F. E.; McIntyre, N. S. ESCA Spectra and Molecular Charge Distributions for Some Pyrimidine and Purine Bases. *Can. J. Chem.* **1978**, *56* (11), 1555−1561.
(56) Wu, X.; Gong, K.; Zhao, G.; Lou, W.; Wang, X.; Liu, W. Mechanical Synthesis of Chemically Bonded Phosphorus−Graphene Hybrid as High-Temperature Lubricating Oil Additive. *RSC Adv.* **2018**, *8*, 4595−4603.
(57) Peng, B.; Xu, Y.; Liu, K.; Wang, X.; Mulder, F. High-Performance and Low-Cost Sodium-Ion Anode Based on a Facile Black Phosphorus−Carbon Nanocomposite. *ChemElectrochem* **2017**, *4*, 2140−2144.
(58) Zha, X.; Hou, X.; Li, Q.; Nan, H.; Ge, F.; Liu, Y.; Li, F.; Zhang, D.; Tian, J. Loading Glyphosate in Attapulgite and Sodium Alginate Hydrogels to Construct PH-Responsive Controlled Release Microsphere for Enhanced Soil Sustained Release. *ACS Agric. Sci. Technol.* **2022**, *2*, 1090.
(59) Knox, H. L.; Sinner, E. K.; Townsend, C. A.; Boal, A. K.; Booker, S. J. Structure of a B12-Dependent Radical SAM Enzyme in Carbapenem Biosynthesis. *Nature* **2022**, *602* (7896), 343−348.
(60) Andexer, J. N.; Richter, M. Emerging Enzymes for ATP Regeneration in Biocatalytic Processes. *ChemBiochem* **2015**, *16* (3), 380−386.
(61) Schümperli, M.; Pellaux, R.; Panke, S. Chemical and Enzymatic Routes to Dihydroxyacetone Phosphate. *Appl. Microbiol. Biotechnol.* **2007**, *75* (1), 33−45.
(62) Kim, D.-M.; Swartz, J. R. Regeneration of Adenosine Triphosphate from Glycolytic Intermediates for Cell-Free Protein Synthesis. *Biotechnol. Bioeng.* **2001**, *74* (4), 309−316.
(63) Clapés, P.; Garrabou, X. Current Trends in Asymmetric Synthesis with Aldolases. *Adv. Synth. Catal.* **2011**, *353* (13), 2263−2283.

https://doi.org/10.1021/acsami.3c19025
ACS Appl. Mater. Interfaces 2024, 16, 11315−11323